

GT2011-45&)

EFFECTS OF MULTIPLE-INJECTION-BURNER CONFIGURATIONS ON COMBUSTION CHARACTERISTICS FOR DRY LOW-NO_x COMBUSTION OF HYDROGEN-RICH FUELS

**Tomohiro Asai, Satoschi Dodo, Hiromi Koizumi, Hirokazu Takahashi,
Shouhei Yoshida, and Hiroshi Inoue**

Energy and Environmental Systems Laboratory
Hitachi, Ltd.
832-2 Horiguchi Hitachinaka-shi, Ibaraki 312-0034 Japan

ABSTRACT

The successful combination of coal-based integrated gasification combined cycle (IGCC) technology with carbon dioxide (CO₂) capture and storage (CCS) requires gas turbines that can achieve dry low-NO_x combustion of hydrogen-rich syngas with a wide range of hydrogen concentrations for lower emissions and higher plant efficiency. The authors have been developing a “multiple-injection burner” to achieve dry low-NO_x combustion of such hydrogen-rich fuels. The purpose of this paper is to experimentally investigate the combustion characteristics of a multiple-injection burner with a convex perforated plate in order to determine its effectiveness in suppressing combustion oscillation. The experiments were conducted at atmospheric pressure. Three kinds of fuel with hydrogen concentrations ranging from 40 to 84% were tested. The temperature of the combustion gas at the burner exit was 1775 K. The experimental results show that the convex burner was effective in suppressing combustion oscillation: it achieved stable low-NO_x emissions of less than 10 ppm for all the test fuels. These findings demonstrate that the convex burner can achieve stable low-NO_x combustion of hydrogen-rich fuels with a wide range of hydrogen concentrations by suppressing combustion oscillation.

INTRODUCTION

Coal-based IGCC technology with CCS will be a necessity for ensuring energy security and mitigating global warming. The energy security of imported-oil-dependent countries is threatened by unstable oil supplies caused by limited reserves, uneven distribution, and rising costs of oil. Coal will become the world’s fossil fuel of choice for ensuring energy security because of its abundant reserves and worldwide availability. Global warming is due to the greenhouse

effect caused by emissions of greenhouse gases (GHG), especially CO₂. The International Energy Agency (IEA) estimates that around 40% of the total CO₂ emissions can be worldwide attributed to power generation [1]. IGCC plants release less CO₂ than conventional pulverized-coal steam plants because of their higher plant efficiency. Another CO₂ reduction method, CCS, prevents the release of CO₂ into the atmosphere by capturing and safely storing CO₂ emissions from power plants. A report by the Intergovernmental Panel on Climate Change (IPCC) estimates that an IGCC plant with CCS may reduce CO₂ emissions by approximately 80–90% compared with an IGCC plant without CCS [2]. The main technical problem associated with CCS, however, is that it reduces plant efficiency owing to the additional energy required for capture and storage. The IPCC report estimates that an IGCC plant with CCS may need 14–25% more energy than an IGCC plant of equivalent output without CCS [2]. This means that improving the efficiency of an IGCC plant with CCS is the key to the successful combination of these two technologies.

In an oxygen-blown IGCC plant with a pre-combustion CO₂ capture system, the hydrogen-rich syngas produced is supplied to a gas turbine as a fuel. The hydrogen concentration of the hydrogen-rich syngas varies from approximately 25 to over 80% depending on the carbon capture rate [3]. Hydrogen poses significant challenges in combustion systems because of its high flame speed, low ignition energy, and broad flammability limits compared with conventional gas-turbine fuels like natural gas. These hydrogen properties increase the risk of flashback and auto-ignition [4, 5]. Conventional premixed combustors, which are highly tuned to operate on low-hydrogen-content fuels like natural gas, cannot achieve stable low-NO_x combustion of hydrogen-rich fuels because of

flashback into their large premixing section. Conventional diffusion-flame combustors cannot achieve higher plant efficiency because of the additional energy required to inject a diluent, such as nitrogen, water, or steam, into the combustion zone of the combustor to suppress the increased NOx emissions. The successful introduction of CCS into IGCC plants requires advanced technologies for dry low-NOx combustion of hydrogen-rich fuels that can achieve both low-NOx emissions and higher plant efficiency. A great deal of research and development on dry low NOx combustion technology for hydrogen-rich fuels has already been done [6–11].

The authors have been developing a “multiple-injection burner” as an advanced concept [11]. This burner consists of multiple fuel nozzles and a flat perforated plate with multiple air holes. At each injection point, one fuel nozzle and one air hole are installed coaxially. At each point, a fuel jet surrounded by a sheath air jet is injected. The burner can lift a flame from the burner by producing a converging-diverging flow just downstream of the burner. Lifting a flame in this manner can reduce the risk of flashback into the burner and reduce NOx emissions. However, stable low-NOx operation is prevented by the occurrence of combustion oscillation [11].

This study suggests a multiple-injection burner with a convex perforated plate for suppressing the combustion oscillation. Its effectiveness for hydrogen-rich fuels with a wide range of hydrogen concentrations was investigated by atmospheric experiment.

HYDROGEN-RICH SYNGAS IN IGCC WITH CCS

Coal-based IGCC with CCS is the technology that converts coal to a syngas, removes CO₂ from the syngas, and generates power in a combined cycle plant by using the resulting hydrogen-rich syngas as the gas-turbine fuel. An oxygen-blown IGCC plant with a pre-combustion CCS system consists of five main components: an air separation unit (ASU), a gasifier, a syngas cleanup unit, a CCS system, and a combined cycle plant (Figure 1).

This plant generates power through the following process. The ASU separates air into oxygen and nitrogen. The gasifier converts coal to a raw syngas by reacting it with a mixture of oxygen and steam under pressure. The syngas cleanup unit removes impurities like sulfur, ammonia, and particulate matter from the raw syngas, producing a clean syngas comprised mainly of carbon monoxide (CO) and hydrogen (H₂). A shift reactor in the CCS system converts CO contained in the clean syngas to H₂ and CO₂ by a water-gasshift reaction, producing a “shifted syngas.” A CO₂ removal unit removes CO₂ from the shifted syngas, producing a hydrogen-rich syngas. The hydrogen-rich syngas is supplied to the gas turbine as a fuel. In the gas turbine, the hydrogen-rich syngas is burned in the combustor, and the combustion gas operates the turbine, which, in turn, generates power. A heat recovery steam generator (HRSG) produces steam using the waste heat from

the gas turbine, sending the steam to the steam turbine, which generates additional power using that steam.

The compositions of the hydrogen-rich syngas supplied to the gas turbine vary widely depending on the carbon capture rate (Table 1). As the carbon capture rate increases from zero to 50 and then 90%, as a result of the conversion of CO to H₂ and CO₂ in the shift reactor, H₂ concentration increases from 26.5 to 83.5%, and CO concentration decreases from 60 to 5%. The flame speed of the syngas increases when the carbon capture rate increases because of the increase in the H₂ concentration of the syngas.

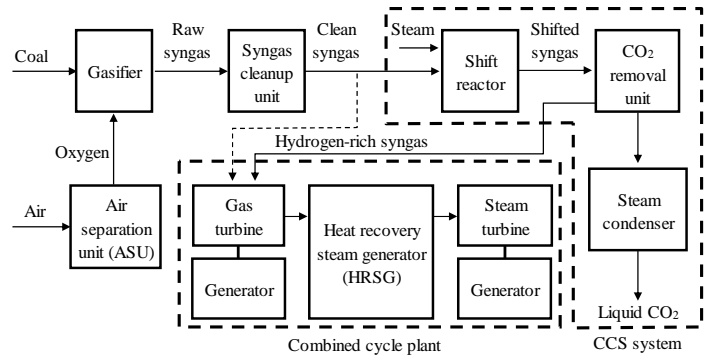


Figure 1. Schematic diagram of oxygen-blown IGCC plant with pre-combustion CCS system.

Table 1. Compositions of hydrogen-rich syngas in IGCC with CCS.

Constituents:		Hydrogen-rich syngas		
		Carbon capture rate		
		0%	50%	90%
H ₂	vol.%	26.5	58.0	83.5
CO	vol.%	60.0	30.5	5.0
CH ₄	vol.%	1.0	1.0	1.0
Other hydrocarbons	vol.%	0.0	0.0	0.0
Inert gas (N ₂ , CO ₂)	vol.%	12.5	10.5	10.5
Density	kg/m ³ *	0.937	0.572	0.276
Lower heating value	MJ/m ³ *	10.8	10.5	10.0
	MJ/kg	11.5	18.3	36.2

* at 273.15 K, 0.1013 MPa

CONCEPT OF MULTIPLE-INJECTION BURNER

This chapter describes the concept of the multiple-injection burner. Figure 2 shows a schematic view of the burner. The conventional multiple-injection burner has a flat perforated plate [11]. The air holes on the perforated plate are arranged in three circles: six holes are arranged on the first circle (with the smallest diameter), 12 holes on the second circle (with the middle diameter), and 18 holes on the third circle (with the largest diameter). Hereafter, the region within the first circle on the perforated plate is called the “inner region” and the region outside the first circle is called the “outer region.” The air holes cause the combustion air passing through them to swirl because the central axis of each hole is

inclined in the direction of a tangent to each of the circles. The burner is connected to a model gas-turbine combustor with a burner body that is equipped with an air inlet and two fuel inlets. The combustion air enters the burner body through the air inlet and then emanates from the air holes into the combustion chamber. Fuel enters the burner body through the two fuel inlets and emanates from the fuel nozzles through the air holes into the combustion chamber. Hereafter, the fuel emanating through the six air holes on the first circle is referred to as “inner fuel” and the fuel emanating through the 30 air holes on the second and third circles is referred to as “outer fuel.” The distribution of the inner and outer fuel affects the combustion characteristics of the burner. The ratio of the flow rate of the outer fuel to that of all the fuel is referred to as the “outer-fuel ratio” hereafter. The outer-fuel ratio is the test parameter in this study.

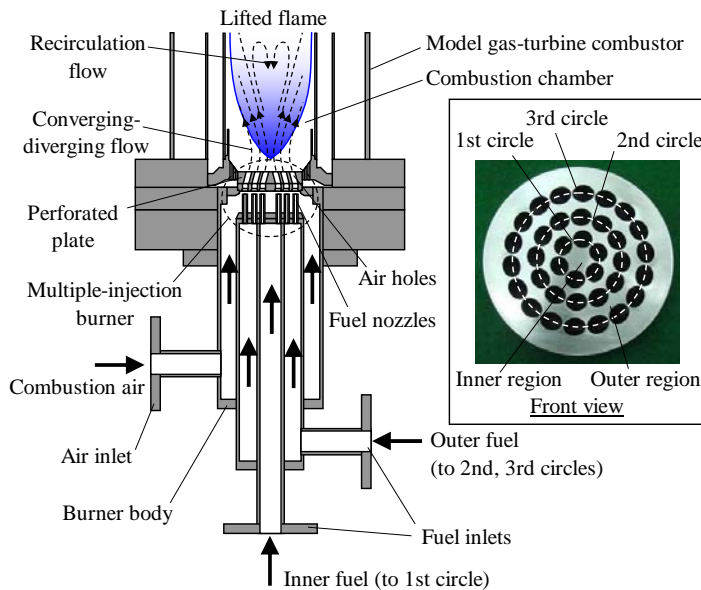


Figure 2. Schematic view of multiple-injection burner.

The concept of the multiple-injection burner operating with hydrogen-rich fuels is to lift a flame from the burner by producing a converging-diverging swirling flow just downstream of the burner. The converging flow generates a favorable pressure gradient, whereas the diverging flow generates an adverse pressure gradient. The favorable pressure gradient can suppress the backflow of the combustion gas from the boundary between the converging flow and the diverging flow. The adverse pressure gradient causes a vortex breakdown on the boundary, thereby producing a recirculation flow for stabilizing the flame and as a result, the flame is stabilized on the boundary. The lifted flame can reduce the risk of flashback into the burner. Moreover, the lifted flame can reduce NO_x emissions because of the enhanced fuel-air mixing due to the increased mixing length. Thus, the burner can achieve stable low-NO_x combustion of hydrogen-rich fuels with a wide range of H₂ concentrations.

The burner can allow stable low-NO_x combustion by achieving homogeneous lean combustion. Homogeneous lean combustion can be achieved by supplying fuel to each fuel nozzle at an equal flow rate. This fuel supply yields an outer-fuel ratio of 83.3%, which equals the proportion of the number of fuel nozzles in the outer region to the total number of fuel nozzles. Hereafter, the outer-fuel ratio of 83.3% is called the “target outer-fuel ratio.” The experimental results showed that NO_x emissions decreased when the outer-fuel ratio increased and NO_x emissions took the minimum values at the target outer-fuel ratio [11].

However, stable low-NO_x operation is prevented by the occurrence of combustion oscillation because the combustion oscillation occurs at a certain outer-fuel ratio below the target ratio when the outer-fuel ratio is increased. The combustion oscillation may be triggered by the attachment of the flame to the outer region on the perforated plate due to the ignition of flammable mixtures in the wake behind the plate. The achievement of stable low-NO_x combustion for the multiple-injection burner requires homogeneous lean combustion due to the increase in the outer-fuel ratio up to the target ratio of 83.3% without the combustion oscillation.

To suppress the combustion oscillation, the authors’ previous study suggested a multiple-injection burner that was equipped with fuel nozzles with a smaller fuel-injection-hole diameter. This burner succeeded in suppressing the combustion oscillation because its higher fuel jet velocity prevented the presence of flammable mixtures in the wake behind the burner by increasing the penetration of the fuel jet into the combustion chamber. However, from the viewpoint of practical application, this burner might pose additional problems for the gasifier in IGCC plants because the smaller fuel-injection-hole diameter increases fuel supply pressure. Thus, another method of suppressing the combustion oscillation is required.

This study suggests a multiple-injection burner with a convex perforated plate as a method of suppressing the combustion oscillation. Figure 3 shows the concept of the burner with the convex perforated plate. The center of the perforated plate projects into the combustion chamber and the surface is inclined. Hereafter, this burner is called the “convex burner.”

The convex burner may be effective in suppressing the combustion oscillation because of the following three effects. The first effect is that the convex burner can suppress the ignition of flammable mixtures in the wake behind the plate by keeping the flame away from the plate. The flammable mixtures may be ignited by the combustion gas from the flame as a heat source. Because the distance from the plate surface to the flame becomes larger than that of the flat perforated plate, the combustion gas from the flame provides the flammable mixtures with less heat. As a result, the convex burner can suppress the ignition of flammable mixtures. Moreover, the convex burner may be effective in reducing NO_x emissions because of the increased mixing length. The second effect is that the convex burner can suppress the ignition of flammable

mixtures by reducing the wake size behind the plate. The wake formed behind the convex plate becomes smaller than that behind the flat plate because the growing wake vortices, which are normal to the inclined surface, are swept away by mixture jet flow. As a result, the convex burner can suppress the ignition of flammable mixtures. The third effect is that the convex burner can suppress the attachment of the flame to the plate by generating the flow along the plate surface. Because the smaller wake vortices allow an outstanding pressure gradient from the outer region to the center of the burner, it enhances the entrainment from the outer region to the center region, thus generating the flow along the plate surface. The flow can blow the approaching flame off the plate surface. As a result, the convex burner can suppress the attachment of the flame to the plate. The convex burner may be effective in suppressing the combustion oscillation because of these three effects.

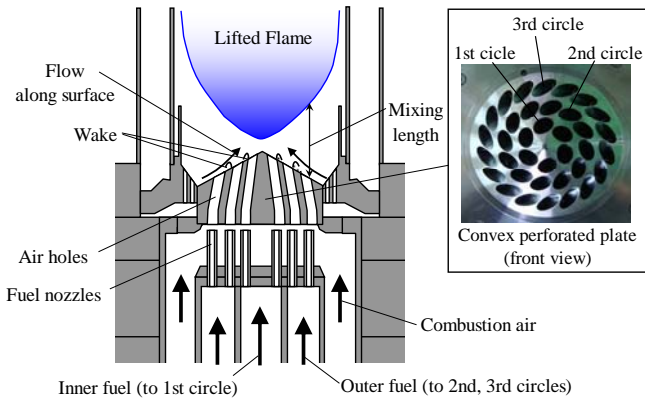


Figure 3. Concept of multiple-injection burner with convex perforated plate.

EXPERIMENTAL APPARATUS AND METHODS

Combustion test rig

The experiments in this study were conducted at atmospheric pressure in a combustion test rig of a model gas-turbine combustor (Figure 4). The main components of the rig are a combustor, air- and fuel-supply systems, and measuring equipment.

The combustor consists of a combustion liner, the multiple-injection burner, and a temperature reducer of the combustion gas. The combustion liner is equipped with five rows of film-cooling air holes and liner lips on the surface and has a cylindrical combustion chamber inside. The burner injects the fuel into the combustion chamber. The fuel mixes and reacts with the combustion air and a flame is then formed in the combustion chamber, thereby generating the combustion gas. The combustion gas flowing through the combustion chamber is discharged into the atmosphere after the combustion gas has been cooled by water spray in the temperature reducer.

The air-supply system supplies combustion air and cooling air separately to the combustor from an air compressor

through a preheater. The combustion air entering the combustion chamber through the burner is used as an oxidant in the combustion. The cooling air entering the combustion chamber through a flow sleeve cools the combustion liner by impinging on its outer surface and flowing along its inner surface. The fuel-supply system independently supplies the constituents of the fuel (H_2 , methane (CH_4), and nitrogen (N_2)) to a gas mixer that produces a gas mixture at certain compositions. The compositions of the gas mixture were varied by independently changing the flow rates of the constituents. The gas mixture is separated into inner fuel and outer fuel. The inner fuel is supplied to the six fuel nozzles on the first circle of the perforated plate and the outer fuel is supplied to the 30 fuel nozzles on the second and third circles.

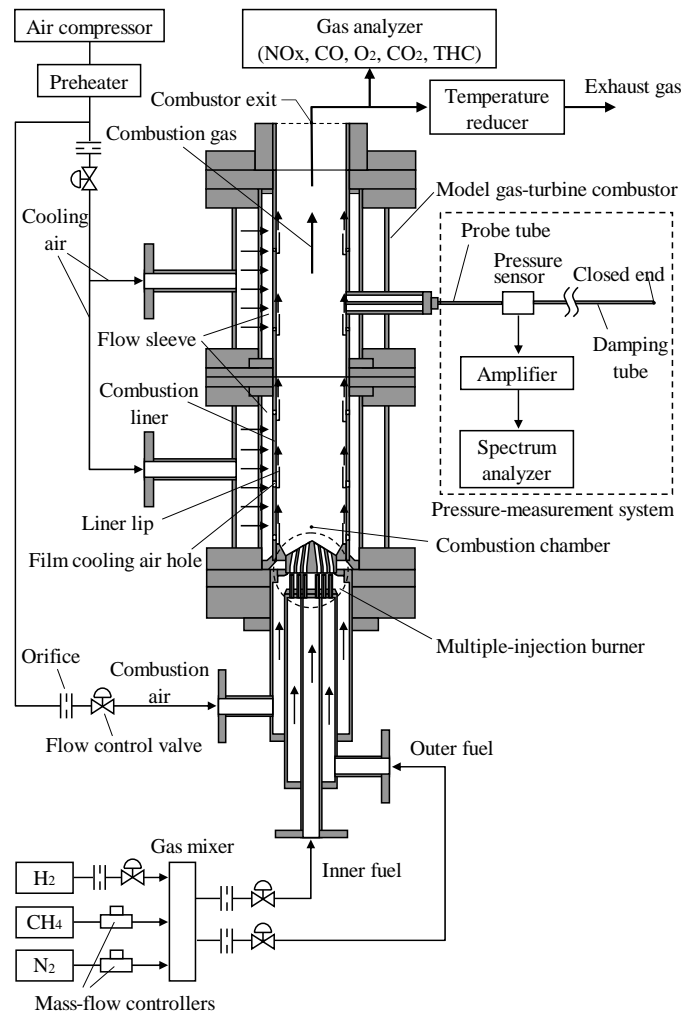


Figure 4. Schematic diagram of combustion test rig.

The measuring equipment consists of a gas analyzer (HORIBA, Ltd., Model VIA-510) and a pressure-measurement system. The gas analyzer measures the concentrations of NOx, CO, O₂, CO₂, and total hydrocarbons (THC) contained in the

combustion gas, which is sampled at a position located in front of the temperature reducer. The pressure-measurement system measures the fluctuation of combustion pressure at a point on the inner surface of the combustion liner. The system consists of a probe tube, a pressure sensor (PCB Piezotronics, Inc., Model S112A21), an amplifier (PCB Piezotronics, Inc., Model 584), a spectrum analyzer (Takeda Riken TR9405A), and a damping tube. The pressure sensor detects pressure fluctuation at the measuring point through the probe tube. It then transmits the signal of the pressure fluctuation to an amplifier, which amplifies the signal and transmits the amplified signal to a spectrum analyzer. The spectrum analyzer calculates the spectrum of the amplified signal. A damping tube with a closed end removes any pseudo signals due to acoustic resonance produced in the probe tube.

Test Burners

Two types of burners were tested in the experiments. Figure 5 shows their configurations. One has a conventional flat perforated plate (Plate A), and the other has a convex perforated plate (Plate B). Both burners are equipped with fuel nozzles with an injection-hole diameter of 3.0 mm. A comparison between the two test burners reveals the effects of the convex perforated plate on the combustion characteristics.

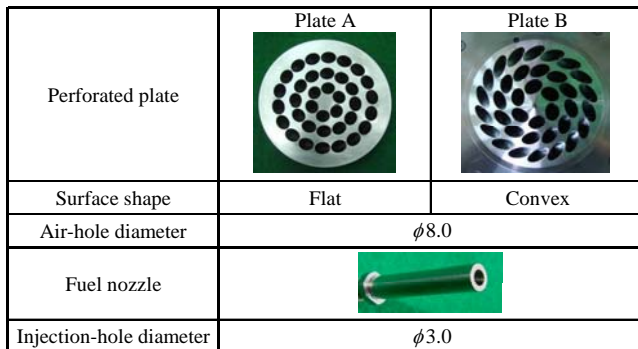


Figure 5. Test burner configurations.

Test fuels

Table 2 lists the compositions of the three test fuels used in the experiments. The test fuels were comprised of three constituents: H_2 , CH_4 , and N_2 . The test fuels had approximately equivalent lower heating values per unit volume to the previously mentioned hydrogen-rich syngas at carbon capture rates of zero, 50, and 90% (see Table 1). Hereafter, the test fuels will be referred to as “CCS-0% fuel,” “CCS-50% fuel,” and “CCS-90% fuel.” H_2 concentration of the test fuels ranged from 40 to 84%, and the lower heating value per unit volume ranged from 9.3 to 10.8 MJ/m³ (at 273.15 K, 0.1013 MPa). The test fuels did not contain CO so that they would have equivalent composition as the fuels used in the tests under actual operating conditions because the supply system used in the tests under actual operating conditions cannot supply CO. A comparison between the test fuels clarifies the effect of the fuel

composition (especially H_2 concentration) on the combustion characteristics.

Table 2. Composition of test fuels.

Test fuels		CCS-0% fuel	CCS-50% fuel	CCS-90% fuel
Constituents:				
H_2	vol.%	40.0	65.0	84.0
CH_4	vol.%	18.0	6.3	2.0
N_2	vol.%	42.0	28.7	14.0
Density	kg/m ³ *	0.690	0.462	0.265
Lower heating value	MJ/m ³ *	10.8	9.3	9.8
	MJ/kg	15.7	20.1	36.9

* at 273.15 K, 0.1013 MPa

Test conditions

The experiments were conducted under the test conditions listed in Table 3. The combustion air-flow rate was kept constant at 157 m³/h (at 273.15 K, 0.1013 MPa). The combustion-air temperature was maintained at 623 K, which was the maximum temperature set for this combustion test rig. The pressure in the combustor was atmospheric pressure. The temperature of the combustion gas at the burner exit, which will be referred to hereafter as the “burner exit-gas temperature,” was 1775 K. The authors’ previous study showed that the combustion oscillation tended to occur at higher burner exit-gas temperatures [11]. The combustion flow at a burner exit-gas temperature of 1775 K was the most subject to the combustion oscillation because this temperature was the highest in the test range.

Table 3. Test conditions.

Combustion-air flow rate:	157 m ³ /h *
Combustion-air temperature:	623 K
Pressure in combustor:	0.1013 MPa
Burner exit-gas temperature:	1775 K

* at 273.15 K, 0.1013 MPa

RESULTS AND DISCUSSION

Flame visualization

The multiple-injection burner can achieve stable low- NO_x combustion of hydrogen-rich fuels by lifting a flame from the burner. Figure 6 shows the typical flame images for CCS-0% fuel in the flat plate (Plate A) and the convex plate (Plate B). These images show that lifted flames were formed above both plates. The distance from the plate surface to the flame for Plate B was larger than that for Plate A (the distances for the second circle are shown as L_A and L_B for Plate A and Plate B, respectively, in the figure.) The larger distance for Plate B may be effective in suppressing the combustion oscillation and reducing NO_x emissions because of the increased mixing length.

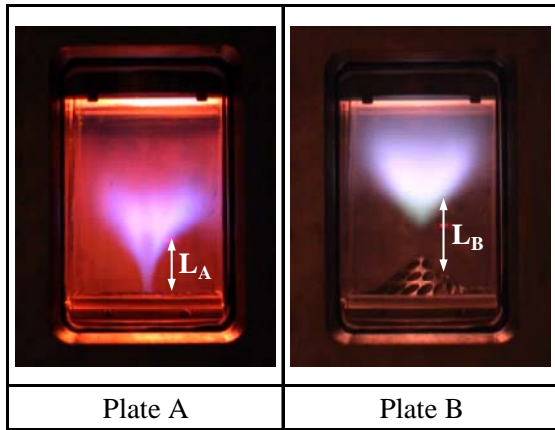


Figure 6. Flame images (CCS-0% fuel).

Effects of convex burner

This section describes the effects of the convex burner by comparing the combustion characteristics of combustion oscillation and NO_x emissions between Plate A and Plate B. The main obstacle to the achievement of stable low-NO_x combustion for the multiple-injection burner is the occurrence of combustion oscillation. Figure 7 shows the spectrum of the pressure fluctuation for Plate A and CCS-0% fuel at an outer-fuel ratio of 85%. The vertical axis expresses the logarithm of the relative amplitude of pressure fluctuation in an arbitrary unit. A distinct single peak appeared at a frequency of 1000 Hz in the spectrum. The combustion oscillation for the multiple-injection burner occurred at a high frequency of around 1000 Hz.

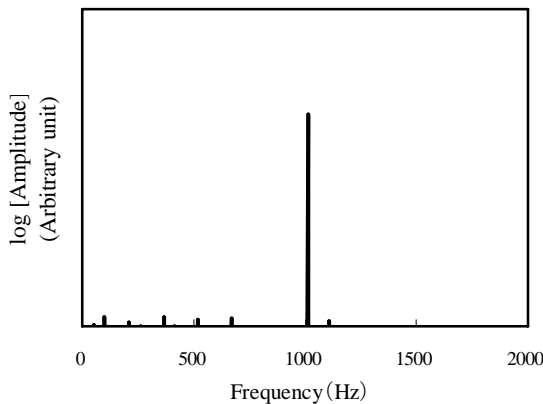


Figure 7. Spectrum of pressure fluctuation (Plate A, CCS-0% fuel, outer-fuel ratio: 85%).

CCS-0% fuel

This subsection compares the combustion characteristics of Plate A and Plate B for CCS-0% fuel. Figure 8 shows the normalized amplitude of pressure fluctuation for CCS-0% fuel as a function of the outer-fuel ratio. The amplitude of pressure

fluctuation was normalized by the criterion for safely operating the burner. Hereafter, this criterion is referred to as the “upper limit.” The combustion oscillation with an amplitude above the upper limit may increase the risk of damage to the burner. An amplitude of zero means that no significant combustion oscillation occurred. The oscillation frequency was 1000 Hz for both plates within the test range of the outer-fuel ratio. This figure shows that the combustion oscillation occurred at outer-fuel ratios above 75.0% for Plate A and above 89.4% for Plate B. The amplitude for Plate B was lower than that for Plate A. The amplitudes for both plates were below the upper limit for CCS-0% fuel. This finding shows that Plate B was effective in suppressing the occurrence of combustion oscillation. This effect is most likely due to the convex surface of Plate B. The convex surface can suppress the ignition of flammable mixtures in the wake and the flame attachment to the burner, which may be the main cause of the combustion oscillation.

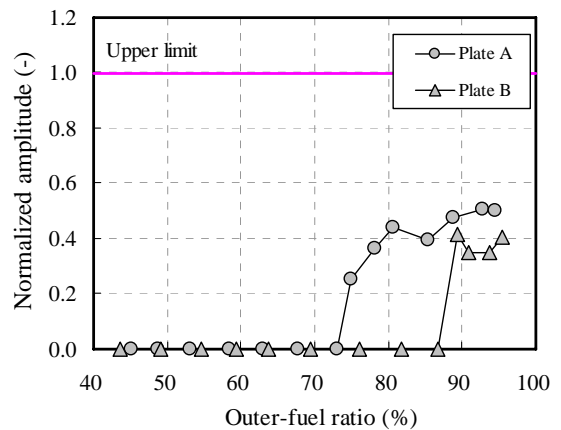


Figure 8. Variations in amplitude of pressure fluctuation with outer-fuel ratio (CCS-0% fuel).

Figure 9 shows the concentration of NO_x emissions for CCS-0% fuel as a function of the outer-fuel ratio. The figure shows that NO_x emissions for both plates decreased when the outer-fuel ratio was increased to below the target ratio (83.3%), and took the minimum values around the target ratio, and then increased when the outer-fuel ratio was increased to above the target ratio. This result shows that homogeneous lean combustion was achieved around the target outer-fuel ratio. The higher NO_x emissions at outer-fuel ratios below and above the target ratio were a result of the formation of flames with a higher equivalence ratio in the inner region and outer region, respectively. The flames with a higher equivalence ratio formed more NO_x because of their high flame temperatures. The NO_x emissions for Plate B were lower than those for Plate A within the test range. The difference in NO_x emissions between Plates A and B may be due to the increase in mixing length. The flame images in Figure 6 show that the distance from the plate surface to the flame for Plate B, L_B, was larger than that for Plate A, L_A. The increase in the distance enhanced the fuel-air mixing and thus reduced NO_x emissions.

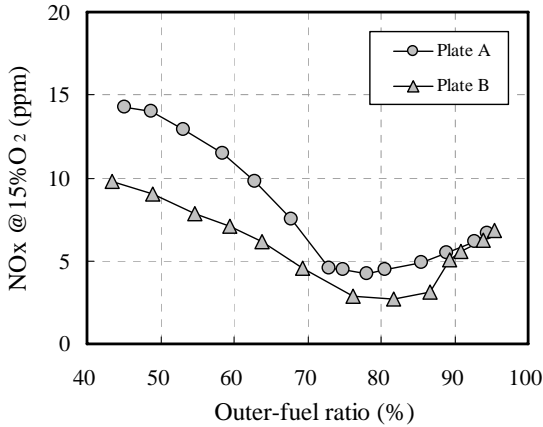


Figure 9. Variations in NOx emissions with outer-fuel ratio (CCS-0% fuel).

Next, the flame holding stability is described. The flame holding stability is evaluated in terms of combustion efficiency as follows. Combustion efficiency η is defined as the ratio of the actual heat energy released in combustion to the theoretical heat energy available. A higher value of combustion efficiency indicates greater flame holding stability. Combustion efficiency is calculated from the expression:

$$\eta = \frac{Q_{in} - Q_{out}}{Q_{in}} \times 100 \quad (1),$$

in which Q_{in} (kJ/m³) denotes the heat energy input for combustion, and Q_{out} (kJ/m³) denotes the heat energy not consumed in combustion. Q_{in} equals the lower heating value of the test fuels per unit volumetric fuel flow rate. Q_{out} is calculated from the expression:

$$Q_{out} = [\text{CO}] \times \text{LHV}_{\text{CO}} + [\text{THC}] \times \text{LHV}_{\text{CH}_4} \quad (2),$$

in which [CO] (vol.%) and [THC] (vol.%) denote the measured concentrations of CO and THC emissions, respectively, contained in the combustion gas; LHV_{CO} (kJ/m³) and LHV_{CH_4} (kJ/m³) denote the lower heating values of CO and CH₄, respectively. Expression (2) did not evaluate the concentration of H₂ contained in the combustion gas because the gas analyzer in the test rig was not able to measure H₂ concentrations. However, effects of the H₂ concentration on combustion efficiency were negligible because the uncertainties due to the exclusion of the H₂ concentration were less than 0.003%. Figure 10 shows the combustion efficiency for CCS-0% fuel as a function of the outer-fuel ratio. The combustion efficiency was above 99.9% for both plates within the test range. Thus, both plates demonstrated sufficient flame holding stability.

From the viewpoint of practical application, the combustor length required for Plate B will be commented on. The flame for Plate B was formed more downstream than that for Plate A (Figure 6). However, utilization of Plate B imposes no requirement on extending the combustor length compared with that for Plate A. The high combustion efficiency for Plate B indicates that complete combustion was attained in the combustor with the same length as that for Plate A. Moreover, stationary gas turbine combustors are generally sufficiently long to achieve a satisfactory and consistent distribution of temperature in the combustion gas discharging into the turbine. Thus, the combustor length for Plate B doesn't need to be extended compared with that for Plate A.

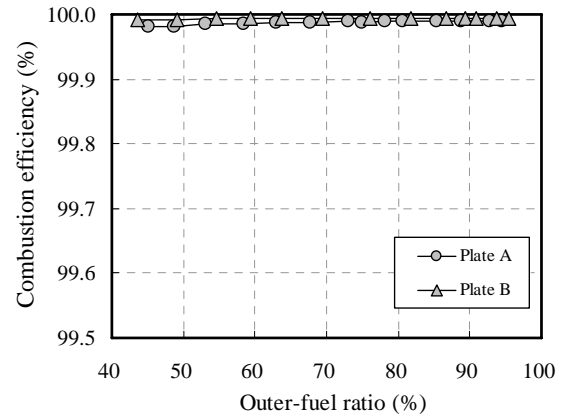


Figure 10. Variations in combustion efficiency with outer-fuel ratio (CCS-0% fuel).

CCS-90% fuel

This subsection compares the combustion characteristics of Plate A and Plate B for CCS-90% fuel. The flame for CCS-90% fuel tends to approach the plate closer because of the higher flame speed. Figure 11 shows the normalized amplitude of pressure fluctuation for CCS-90% fuel as a function of the outer-fuel ratio. The oscillation frequency was 1080 Hz for both plates within the test range. This figure shows that the combustion oscillation emerged at the outer-fuel ratio of 52.6% for both plates. However, the amplitude for Plate A exceeded the upper limit at outer-fuel ratios above 56.2%, and thus the outer-fuel ratio could not increase above this ratio. In contrast, the amplitude for Plate B was below the upper limit within the test range and thus increased up to the target ratio. This finding shows that Plate B was effective in suppressing the combustion oscillation for CCS-90% fuel as well.

The combustion oscillation emerged at lower outer-fuel ratios for CCS-90% fuel than for CCS-0% fuel. This is most likely due to the higher flame speed for CCS-90% fuel. The flame approached closer, and thus the combustion oscillation tended to occur.

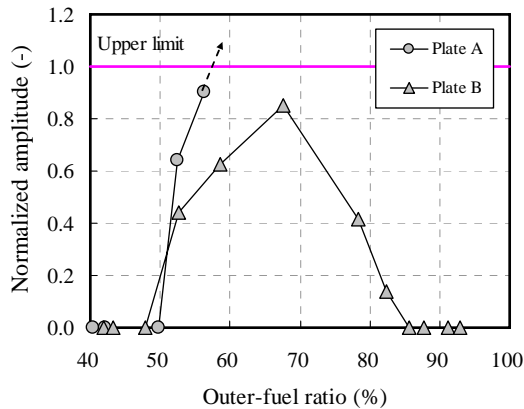


Figure 11. Variations in amplitude of pressure fluctuation with outer-fuel ratio (CCS-90% fuel).

Figure 12 shows the concentration of NOx emissions for CCS-90% fuel as a function of the outer-fuel ratio. The minimum value of NOx emissions for Plate A was 31.6 ppm at the outer-fuel ratio of 56.2% because the amplitude of pressure fluctuation exceeded the upper limit at outer-fuel ratios above this ratio. In contrast, the minimum value of NOx emissions for Plate B was 6.5 ppm at the target outer-fuel ratio of 83.3%. Therefore, Plate B reduced NOx emissions by increasing the outer-fuel ratio up to the target ratio.

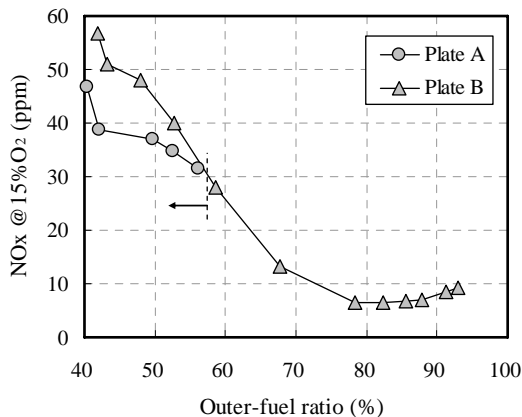


Figure 12. Variations in NOx emissions with outer-fuel ratio (CCS-90% fuel).

NOx characteristics of convex burner

The previous section described how the convex burner was effective in suppressing the combustion oscillation, thus reducing NOx emissions. This section describes in detail the NOx characteristics of the convex plate. Figure 13 shows the effect of fuel composition on variations in concentration of NOx emissions as a function of the outer-fuel ratio for CCS-0, 50, and 90% fuels. The figure shows that the variations in NOx

emissions had the same tendency for each fuel. NOx emissions decreased with increasing the outer-fuel ratio to below the target ratio of 83.3%, and took the minimum values at the target ratio, and then increased when the outer-fuel ratio was increased to above the target ratio. However, NOx emissions increased when CCS increased at an outer-fuel ratio within the test range. This increase is most likely caused by the approach of the flame to the plate and by the increase in the flame temperature when H₂ concentration in the fuel increased. The flame speed increases with the H₂ concentration in fuel, and thus the flame comes closer to the plate. Consequently, the NOx-generating flame zone expands into the neighborhood of the burner and the fuel-air mixing length from the burner to the flame front decreases, thereby increasing NOx emissions. Moreover, the flame temperature increases with the H₂ concentration, which also increases NOx emissions.

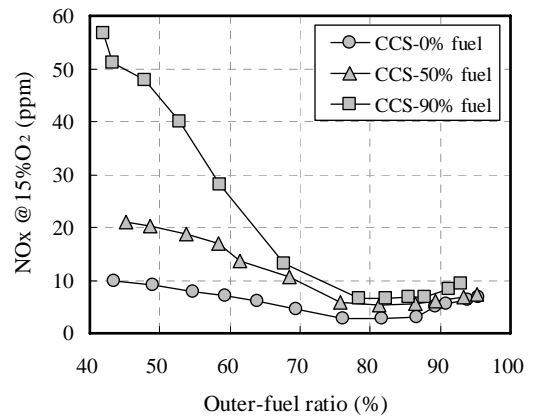


Figure 13. Effect of fuel composition on variations in NOx emissions with outer-fuel ratio (Plate B).

Figure 14 shows the variations in NOx emissions at the target outer-fuel ratio with the carbon capture rate. The NOx emissions at the target ratio were the minimum values for each fuel. The figure shows that NOx emissions at the target ratio increased when the carbon capture rate increased. The NOx emissions at the target ratio were 2.7, 5.3, and 6.5 ppm for CCS-0, 50, and 90% fuels, respectively. However, NOx emissions were less than 10 ppm for all fuels. This finding demonstrates that the convex burner achieved stable low-NOx combustion of hydrogen-rich fuels with H₂ concentration ranging from 40 to 84%.

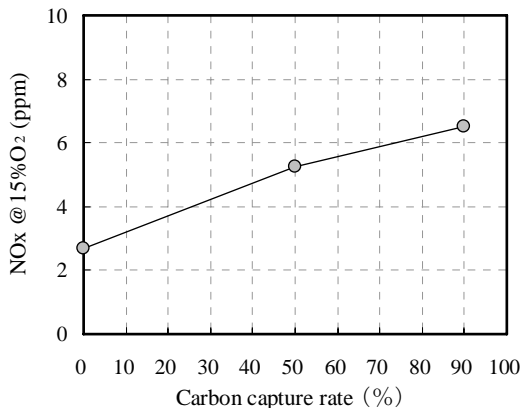


Figure 14. Variations in NOx emissions at target outer-fuel ratio with carbon capture rate (Plate B).

SUMMARY

This paper experimentally investigated the combustion characteristics of the multiple-injection burner with the convex perforated plate in order to determine the burner's effectiveness in suppressing combustion oscillation for stable low-NOx combustion of hydrogen-rich fuels with a wide range of hydrogen concentrations. The two main findings from these experiments at atmospheric pressure are summarized as follows.

- The convex burner was effective in suppressing the combustion oscillation for CCS-0, 50, and 90% fuels.
- The convex burner achieved NOx emissions of 2.7, 5.3, and 6.5 ppm for CCS-0, 50, and 90% fuels at the target outer-fuel ratio. This burner achieved stable low-NOx emissions of less than 10 ppm for hydrogen-rich fuels containing 40–84% hydrogen.

In conclusion, the convex burner can achieve stable low-NOx combustion of hydrogen-rich fuels with a wide range of hydrogen concentrations at atmospheric pressure by suppressing the combustion oscillation.

Further studies are required to apply the multiple-injection burner to dry low-NOx combustors on hydrogen-rich fuels. First, the performance of the burner at higher pressures must be investigated. The flame tends to approach the burner closer at higher pressures under actual operating conditions in a gas turbine combustor because of the higher flame speed. This flame behavior may cause combustion oscillation, increase NOx emissions, and increase metal temperature of the burner. The application of the burner requires the demonstration of its ability to alleviate these problems at higher pressures. Second, the appropriate integration of the burner into dry low-NOx

combustors must be demonstrated. To demonstrate it, the authors have been developing combustors equipped with the multiple-injection burners. The combustors are equipped with a pilot multiple-injection burner at the center and some main multiple-injection burners around the pilot burner. The authors have been investigating the combustor's performance under medium pressure [12].

ACKNOWLEDGMENTS

This work was done for a project carried out by the New Energy and Industrial Technology Development Organization (NEDO), "Innovative Zero-emission Coal Gasification Power Generation Project: Development of Low NOx Combustion Technology for High-Hydrogen Syngas in IGCC". The authors would like to thank NEDO for entrusting the project to us.

REFERENCES

- [1] International Energy Agency (IEA), 2009, "CO₂ Emissions from Fuel Combustion Highlights (2009 edition)," Paris, France.
- [2] Intergovernmental Panel on Climate Change (IPCC), 2005, "IPCC Special Report on Carbon Dioxide Capture and Storage," edited by Metz, B., Davidson, O., Coninck, H., Loos, M., and Meyer, L., Cambridge University Press, New York, USA.
- [3] New Energy and Industrial Technology Development Organization (NEDO), 2005, "Report (FY2004) in Clean Coal Technology Promotion Program: Investigation for Co-production System Based on Coal Gasification," No.100005208, NEDO, Kawasaki, Japan (in Japanese).
- [4] McDonell, V., 2006, "Key Combustion Issues Associated with Syngas and High-Hydrogen Fuels," The Gas Turbine Handbook, USA, Chap. 3.1.
- [5] Jaeger, H., 2007, "Hydrogen-fired Gas Turbine is Key to the Future of IGCC," *Gas Turbine World: May-June*, pp. 29–35.
- [6] GE Energy, 2005, "Final Report: Premixer Design for High Hydrogen Fuels," DOE Cooperative Agreement No. DE-FC26-03NT41893, DOE, Washington, DC, USA.
- [7] Precision Combustion, Inc. (PSI), 2007, "Technical Brief: Fuel Flexibility of Rich Catalytic Lean burn (RCL[®]) System," <http://www.precision-combustion.com/atcc.html>.
- [8] Lee, H., Hernandez, S., McDonell, V., Steinthorsson, E., Mansour, A., and Hollon, B., 2009, "Development of Flashback Resistant Low-Emission Micro-Mixing Fuel Injector for 100% Hydrogen and Syngas Fuels," GT2009-59502, *Proceedings of ASME Turbo Expo 2009*, Orlando, Florida, USA.
- [9] Smith, K., Therkelsen, P., Littlejohn, D., Ali, S., and Cheng, R., 2010, "Conceptual Studies of a Fuel-Flexible Low-Swirl Combustion System for the Gas Turbine in Clean Coal Power Plants," GT2010-23506, *Proceedings of ASME Turbo Expo 2010*, Glasgow, UK.
- [10] Lammel, O., Schütz, H., Schmitz, G., Lücknerath, R., Stöhr, M., Noll, B., Aigner, M., Hase, M., and Krebs, W., 2010,

“FLOX[®] Combustion at High Power Density and High Flame Temperatures,” GT2010-23385, *Proceedings of ASME Turbo Expo 2010*, Glasgow, UK.

- [11] Asai, T., Koizumi, H., Dodo, S., Takahashi, H., Yoshida, S., and Inoue, H., 2010, “Applicability of a Multiple-Injection Burner to Dry Low-NO_x Combustion of Hydrogen-Rich Fuels,” GT2010-22286, *Proceedings of ASME Turbo Expo 2010*, Glasgow, UK.
- [12] Dodo, S., Asai, T., Koizumi, H., Takahashi, H., Yoshida, S., and Inoue, H., 2011, “Combustion Characteristics of a Multiple-Injection Combustor for Dry Low-NO_x Combustion of Hydrogen-Rich Fuels under Medium Pressure,” GT2011-45459, *Proceedings of ASME Turbo Expo 2011*, Vancouver, Canada.